nature biotechnology

# Fluorogen-activating single-chain antibodies for imaging cell surface proteins

Christopher Szent-Gyorgyi[1], Brigitte A Schmidt[1], Yehuda Creeger[1], Gregory W Fisher[1], Kelly L Zakel[1], Sally Adler[2], James A J Fitzpatrick[1], Carol A Woolford[2], Qi Yan[2], Kalin V Vasilev[2], Peter B Berget[2], Marcel P Bruchez[1,3], Jonathan W Jarvik[2] & Alan Waggoner[1]



**Imaging of live cells has been revolutionized by genetically encoded fluorescent probes, most famously green and other fluorescent proteins, but also peptide tags that bind exogenous fluorophores[1]. We report here the development of protein reporters that generate fluorescence from otherwise dark molecules (fluorogens). Eight unique fluorogen activating proteins (FAPs) have been isolated by screening a library of human single-chain antibodies (scFvs) using derivatives of thiazole orange and malachite green. When displayed on yeast or mammalian cell surfaces, these FAPs bind fluorogens with nanomolar affinity, increasing green or red fluorescence thousands-fold to brightness levels typical of fluorescent proteins. Spectral variation can be generated by combining different FAPs and fluorogen derivatives. Visualization of FAPs on the cell surface or within the secretory apparatus of mammalian cells can be achieved by choosing membrane permeant or impermeant fluorogens. The FAP technique is extensible to a wide variety of nonfluorescent dyes.**

The past 15 years have seen two approaches to building genetically expressible fluorescent tools for live cell studies. Green fluorescent protein and its relatives have been improved by directed evolution, and adapted for use as reporters of protein location and abundance[2], sensors of physical environment properties[3] and energy-transfer reagents to monitor protein-protein interactions and conformational changes[4]. Several site-specific chemical labeling systems have also been devised, broadly grouped into fluorophores that directly bind small peptide motifs, and fluorophores that are conjugated to small molecules that bind to acceptor peptides, either directly or by enzymatic action[5–13]. Chemical labeling systems have been applied as protein location and abundance reporters and as energy-transfer reagents[7].

Fluorophore-small-molecule conjugates like the Snap-tag[11] and Halotag[13] reagents bind acceptor sites specific to the small molecule; in these systems the behavior of the fluorophore is generally not modulated by the act of binding. In contrast, fluorophore behavior may be dynamically altered when directly binding to a peptide. To date this potential has been exploited mainly in the biarsenical system, where binding of FlAsH and ReAsH fluorogens to a tetracysteine motif elicits large enhancements of respective green and red fluorescence[6]. Although directed evolution has altered tetracysteine context to improve binding affinity and quantum yield and reduce cytotoxicity[7], biarsenical functionality largely reflects the rational design of fluorogen and binding site.

Our goal in this study is to extend the fluorogen concept to a broad new class of protein-dye reporters. We seek to exploit immune diversity to isolate multiple peptides that interact differently and dynamically with a given fluorogen and its derivatives. The interplay of these proteins and fluorogens determine the spectral and binding properties. Unlike fluorescent proteins, the reversibly bound fluorophore is directly accessible to experimentation and its chemistry can be modified to alter reporting and sensing capabilities. Besides offering potential as a platform for biosensors, the fluorogenic antibody technology we describe has immediate applications in fluorescence microscopy and cytometry, enabling selective visualization of cell surface and secretory pathway proteins by simply adding fluorogen.

We isolated scFvs that elicited intense fluorescence enhancement from two structurally unrelated dyes, thiazole orange (TO) and malachite green (MG) (**Fig. 1a**). Human scFvs were chosen because they are relatively small (<30 kDa) molecules that retain the wide range of antigen recognition capabilities of the humeral immune system, and are also amenable to use as recombinant tags in fusion proteins. A complex human scFv library composed of $\sim 10^9$ synthetically recombined heavy and light chain variable regions was available in a yeast surface-display format[14], enabling us to use fluorescence-activated cell sorting (FACS) to directly screen for fluorogenic binding to the dyes.

TO and MG are known fluorogens; strong fluorescence activation has been observed when TO intercalates into DNA (550-fold[15]) or when MG binds to a specific RNA aptamer (2,360-fold[16]). Enhanced fluorescence is thought to occur because rapid rotation around a single bond within the chromophore is constrained upon binding. Enhanced fluorescence of such 'molecular rotors' has also been reported for an antibody-dye complex, although with much smaller increases[17].

A sulfonated derivative of TO was synthesized (TO1) that reduced background binding to DNA and increased solubility. TO1 and

[1]Molecular Biosensor and Imaging Center, [2]Department of Biological Sciences, [3]Department of Chemistry, Carnegie Mellon University, 4400 Fifth Avenue, Pittsburgh, Pennsylvania 15213, USA. Correspondence should be addressed to C.S.-G. (css@andrew.cmu.edu) or A.W. (waggoner@andrew.cmu).

Received 16 July; accepted 3 December; published online 23 December 2007; doi:10.1038/nbt1368

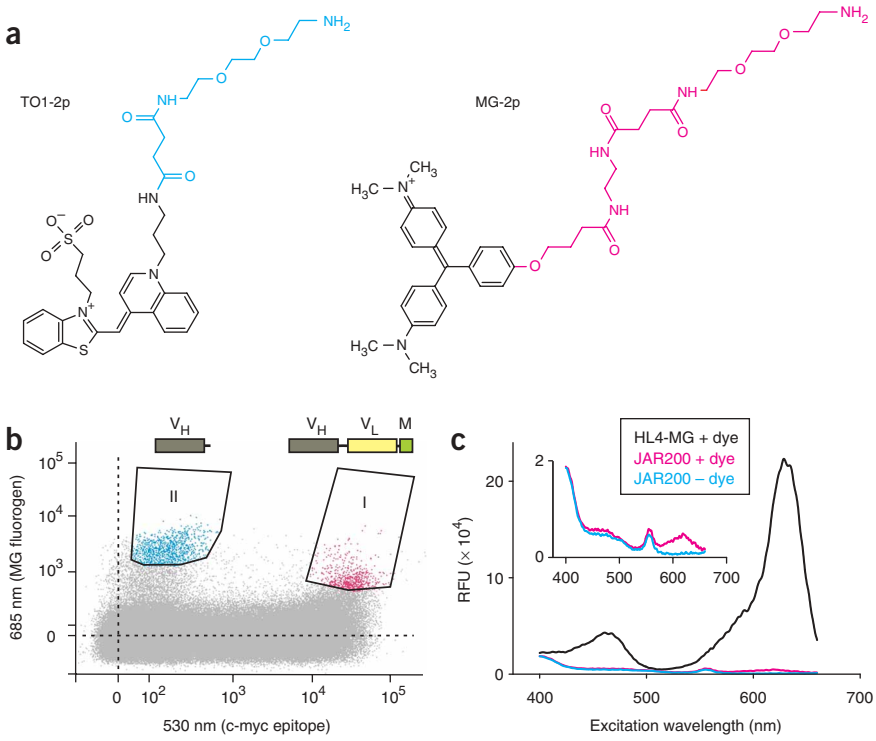


**Figure 1** Fluorogens and their use with yeast-displayed scFvs. (**a**) Structure of fluorogenic dyes used in this study. Depicted are the thiazole orange derivative TO1-2p and the malachite green derivative MG-2p. Dye cores are shown in black and R-group substituents in color. An MG-11p analog of MG-2p was used in some experiments. (**b**) Isolation of FAPs using FACS. Sorting screen shows separation of yeast cells bearing malachite green–activating scFvs from bulk yeast population. Horizontal axis shows distribution of cells by green fluorescence of antibody reagent that labels the c-myc epitope; vertical axis depicts distribution of cells by red fluorescence generated by binding of MG fluorogen. Sorting window (I) collects cells enriched for FAPs composed of heavy chain ($V_H$), light chain ($V_L$) and c-myc epitope (M); window (II) collects cells enriched for FAPs composed only of the heavy chain. (**c**) Homogenous format assay of live yeast cells displaying FAPs. Fluorescence excitation spectrum of displayed HL4-MG taken on 96-well microplate reader; $10^7$ yeast cells in 200 µl (effective concentration ~10 nM scFv) were treated with 200 nM MG-2p. Inset shows low level of fluorescence background signal with JAR200 control cells that do not express FAPs.

MG were coupled to 3,350 or 5,000 MW polyethylene glycol (PEG)-biotin (**Fig. 1a**), and the dye-PEG-biotin conjugates were used with streptavidin and anti-biotin magnetic beads to affinity enrich the yeast surface display library for dye-binding scFvs[18]. The TO1 and MG enriched scFv libraries were further enriched and then screened for fluorescence-generating scFvs by 2-4 rounds of FACS using the dye-PEG conjugates (**Fig. 1b**)[14]. For most subsequent studies, TO1 and MG were coupled to diethylene glycol diamine (TO1-2p and MG-2p, **Fig. 1a**) to maintain the antigenic structure and aqueous solubility.

Sixteen clones that enhanced MG-2p fluorescence and two clones that enhanced TO1-2p fluorescence were isolated from the library (**Supplementary Table 1** online). Sequence analysis has revealed that the TO1-2p FAPs are canonical 2-domain scFvs encoded by different heavy and light chain germline genes[19]. In contrast, the MG-2p scFvs represented six germline configurations, three composed of the usual heavy and light chain segments, and three composed of only a single heavy or light chain segment (**Table 1**). The smallest module, L5-MG, was just 110 amino acids long without the surrounding epitope tags, less than half the size of GFP.

We found that when FAPs were expressed on the yeast cell surface, high quality fluorescence spectra of cell populations could be determined in 96-well plates by direct addition of fluorogen (**Fig. 1c**). We used these homogenous assays to determine binding curves and spectra for all of our FAPs (**Table 1**). Each of the MG FAPs bound MG-2p tightly when assayed on the yeast cell surface, with apparent cell surface dissociation constants in the low nanomolar range. The $K_D$s of HL1-TO1 and HL2-TO1 were in the high nanomolar range. To obtain stronger binders, one of the clones (HL1-TO1) was affinity matured by directed evolution using FACS selection[20] for increased fluorescence at low fluorogen concentration, generating several FAPs with significantly improved brightness and binding affinity (**Supplementary Fig. 1** online). The most improved FAP, HL1.0.1-TO1, bound TO1-2p with a cell surface $K_D$ of about 3 nM.

HL1.0.1-TO1 and HL2-TO1 showed modest red shifts of excitation maxima (509 and 516 nm, respectively) relative to peak free dye absorbance (504 nm), but emission maxima differed more significantly (530 and 550 nm). Cell surface spectra of FAP/MG-2p complexes showed substantial variation. Excitation maxima of the complexes ranged from 620–640 nm, markedly to the red of free dye absorbance (607 nm), whereas emission maxima ranged from 645–670 nm, suggesting an increase in chromophore conjugation length or a correlated quantum yield increase.

To more rigorously investigate the properties of FAP/fluorogens, we produced secreted FAPs and purified the proteins (**Supplementary Fig. 2** online). **Figure 2a** shows fluorescence spectra of these FAPs complexed TO1-2p or MG-2p. In solution, HL1.0.1-TO1 bound TO1-2p with a $K_D$ very similar to that observed on the cell surface (**Table 1** and **Supplementary Fig. 3** online). Direct measurement showed that the fluorescence of TO1-2p increased about 2,600-fold upon binding to the HL1.0.1-TO1. The extinction coefficient and quantum yield of the HL1.0.1-TO1/TO1-2p complex ($\varepsilon$ = 60,000 $M^{-1}cm^{-1}$ and $\Phi$ = 0.47) are comparable to the values for *Aequorea* EGFP (53,000 and 0.60 (ref. 21)), and predict that this FAP/fluorogen has EGFP-like brightness.

HL4-MG and L5-MG respectively showed 185- and 265-fold reduced affinity for MG-2p in solution as compared to surface display, but affinity of H6-MG was reduced only fivefold. We have yet to determine the mechanism of this contrasting behavior. H6-MG binds MG-2p more tightly and with greater quantum yield ($K_D$ = 38 nM, $\Phi$ = 0.25) than the RNA aptamer binds MG ($K_D$ = 117 nM, $\Phi$ = 0.187 (ref. 16)). Our result reflects a fluorescence enhancement of about 18,000-fold as compared to free fluorogen, which is much greater than the 40- to 100-fold enhancement with other antibody/fluorogen complexes[9,17,22] but less than the 50,000-fold increase with a FlAsH reagent[6]. Absorbance of H6-MG/MG-2p is about 1.4-fold greater than free MG-2p (**Table 1** and **Supplementary Fig. 4** online) corresponding to an extinction coefficient of ~105,000 $M^{-1}cm^{-1}$. The

**Table 1 Properties of fluorogen-activating proteins**

| Fluorogen[a] | Fluorogen activating protein | scFv format | scFv size (kDa) | Excitation maximum (nm) | Emission maximum (nm) | Cell surface $K_D$ (nM) | Solution $K_D$ (nM) | Extinction coefficient ($M^{-1}cm^{-1}$) | Quantum yield (Φ) | Fluorescence enhancement |
|---|---|---|---|---|---|---|---|---|---|---|
| **TO1-2p** | **HL1-TO1** | $V_H$-$V_L$ | 26.1 | 510 | 527 | 360 | | | | |
| ε = 58,000 $M^{-1}cm^{-1}$ | **HL2-TO1** | $V_H$-$V_L$ | 26.3 | 516 | 550 | 600 | | | | |
| at 504 nm | **HL1.0.1-TO1** | $V_H$-$V_L$ | 25.9 | 509 | 530 | 3.1 | 1.7 | 60,000 | 0.47 | 2,600 |
| **MG-2p** | **HL4-MG** | $V_H$-$V_L$ | 26.1 | 629 | 649 | 3.2 | 590 | 133,000 | 0.16 | 15,700 |
| ε = 74,250 $M^{-1}cm^{-1}$ | **L5-MG** | $V_L$ | 11.5 | 640 | 668 | 1.2 | 320 | 103,000 | 0.048 | 4,100 |
| at 607 nm | **H6-MG** | $V_H$ | 14.4 | 635 | 656 | 7.5 | 38 | 105,000 | 0.25 | 18,000 |
| | **HL7-MG** | $V_H$-$V_L$ | 26.5 | 619 | 647 | 0.58 | | | | |
| | **H8-MG** | $V_H$ | 13.6 | 626 | 646 | 9.4 | | | | |
| | **HL9-MG** | $V_H$-$V_L$ | 27.9 | 621 | 650 | 0.74 | | | | |

[a]Data for fluorogen at absorbance maximum. Spectral and binding properties determined for fluorogen bound to indicated fluorogen activating protein.

combined absorbance and quantum yield predict a red fluorescent probe with brightness slightly greater than the improved RFP monomer mCherry[23] and slightly less than ReAsH[6]. Excitation/emission fall nearly 50 nm to the red of mCherry and ReAsH, and also to the red side of heme excitation/emission, making this FAP especially well suited for 633 nm laser-excited imaging of mammalian cells and tissue.

Analyses using a variety of chemical derivatives of malachite green revealed that different fluorogen-FAP combinations have different binding affinities, fluorescence intensities and excitation/emission spectra. **Figure 2b** shows the spectral differences produced by three different MG fluorogen derivatives interacting with the same FAP, and shows that the range of variation was specific to a given FAP. Although we do not yet know the specific molecular basis for any of these differences, it is clear that their existence highlights an advantage of our system—namely that one can get different spectral readouts from the same FAP reporter by using different fluorogens.

The FAP-fluorogen system allows for multicolor imaging of cells expressing different FAPs (**Fig. 3a** and **Supplementary Fig. 5** online). We took advantage of the fact that MG and most of its derivatives have a well-resolved secondary excitation peak at near-ultraviolet to blue wavelengths that is sensitive to fluorogenic modulation by the FAP (**Fig. 2b**). We exploited this property to demonstrate fluorescent reporting in non-overlapping green and red colors singly excited by the 488 nm argon laser. The experiment showed that there was no cross-specificity between TO1-2p and MG-2p FAPs, and that in the absence of FAPs neither fluorogen elicited significant fluorescence.

Our yeast FAPs are fused via AGA2 to the AGA1-AGA2 complex, which is directed to the outer leaflet of the plasma membrane by a C-terminal glycosylphosphatidylinositol (GPI) anchor before

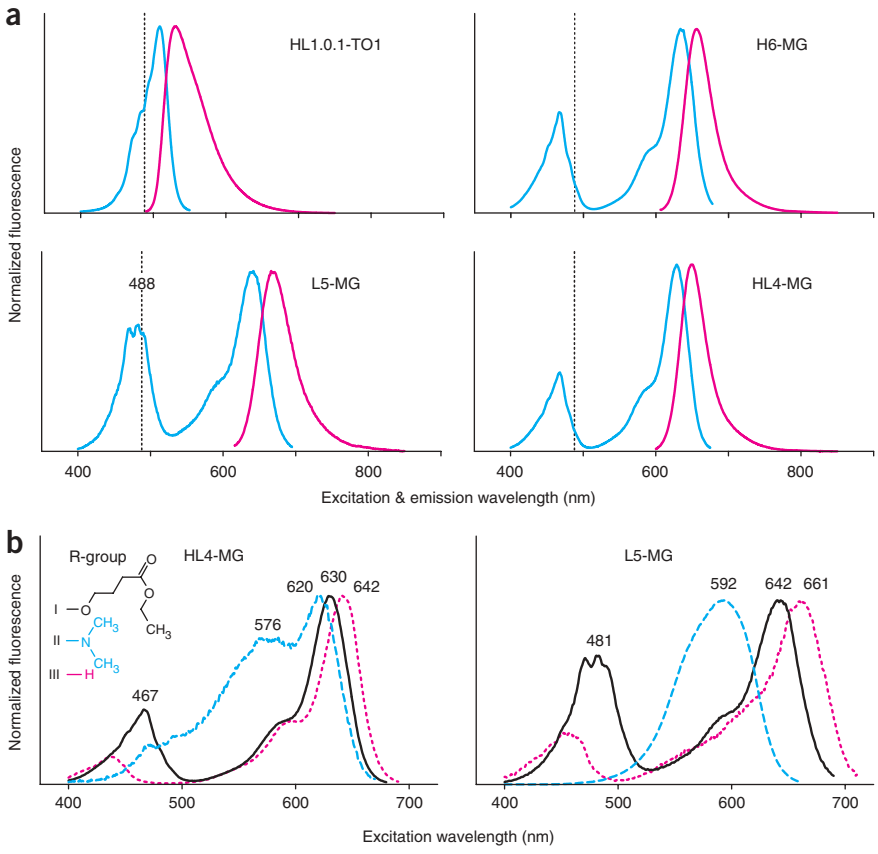


**Figure 2** Fluorescence characterization of purified FAPs. (**a**) Fluorescence spectra of FAP/fluorogen complexes. Excitation and emission spectra were determined in the presence of excess purified FAP (2 μM HL1.0.1-TO1 and 100 nM TO1-2p; 2 μM HL4-MG, L5-MG, H6-MG and 200 nM MG-2p). The 488-nm laser excitation used in the experiment of **Figure 3a** is shown as a dotted line. (**b**) Fluorescence spectra of FAP-fluorogen complexes using different fluorogen analogs; depicted R-groups replace MG-2p R-group in **Figure 1**. Excitation spectra were determined using 2 μM purified HL4-MG or L5-MG and 200 nM of indicated fluorogen analog: (I) malachite green diethylester; (II) crystal violet; (III) malachite green. Fluorescence intensity is normalized; actual fluorescence signal varied, mainly owing to differences in binding affinity. Depicted FAP-fluorogen complexes showed 70- to 12,000-fold fluorescence enhancement over free fluorogen.

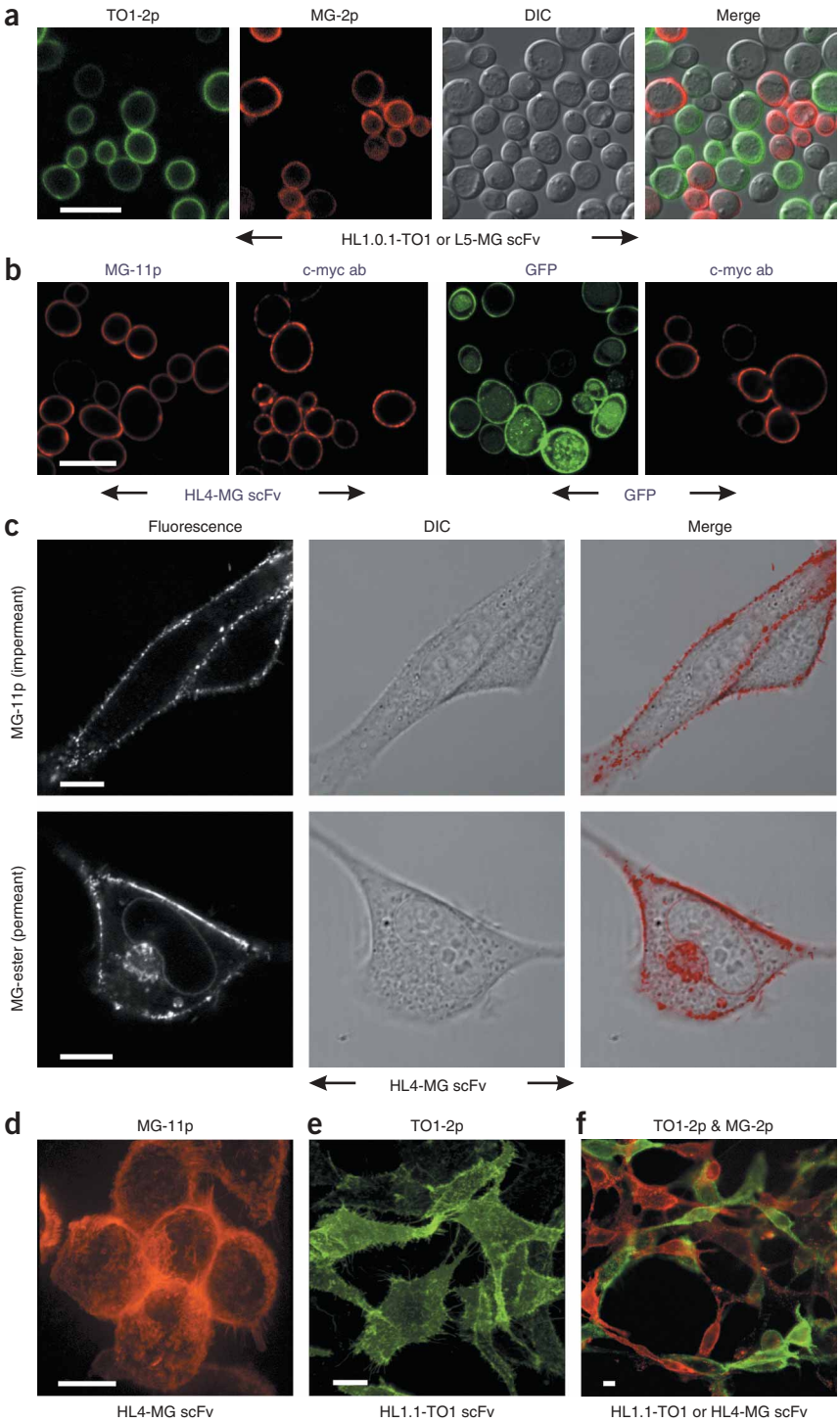


**Figure 3** Fluorescence microscopy of FAPs displayed on live cells. (**a**) Two-color confocal visualization of yeast surface–displayed FAPs using single laser excitation. Cells expressing HL1.0.1-TO1 or L5-MG were mixed 1:1 and excited at 488 nM in the presence of 1 μM TO1-2p and 1 μM MG-2p. Left to right: TO1-2p emission channel (517–583 nm), MG-2p emission channel (668–700 nm), differential interference contrast (DIC) image and merge of fluorescent and DIC images. Statistical analysis indicates no cross-labeling of cell populations. Unlabeled yeast cells that did not express FAPs occured in all populations due to loss of low copy expression plasmid and serve as a control. (**b**) Selective confocal imaging of cell surface by FAPs as compared to GFP. Isogenic yeast strains displaying AGA2-HL4-MG and AGA2-GFP protein fusions were used. As surface labeling controls, c-myc epitopes on the FAP and the GFP were visualized with antibody/second antibody-Alexa 647. Left to right: HL4-MG visualized with 100 nM MG-11p, HL4-MG c-myc control, GFP native fluorescence, GFP c-myc control. (**c**) Selective visualization of biosynthetic-secretory compartment using membrane permeant fluorogen. NIH3T3 cells stably expressing HL4-MG fused to PDGFR were imaged by confocal microscope at 633 nm excitation after treatment for 5 min in PBS with 200 nM MG-11p (top row, membrane impermeant) or 200 nM MG-ester (bottom row, membrane permeant; for structure see **Fig. 2b** R-group I). On longer incubation, MG-ester illuminated intracellular features such as the nuclear periphery (endoplasmic reticulum) and Golgi become more difficult to visualize. (**d**) Surface labeling of human tumor cells with a MG FAP. Stably transformed M21 melanoma cells expressing HL4-MG fused to PDGFR were imaged as a confocal stack at 488-nm excitation using 10 nM MG-11p. Photomicrograph is a three-dimensional reconstruction of the stack. (**e**) Surface labeling of fibroblasts with a TO1 FAP. Stably transformed NIH3T3 cells expressing HL1.1-TO1 fused to PDGFR and imaged as in **d** using 40 nM TO1-2p. (**f**) Simultaneous surface labeling of fibroblasts with MG and TO1 FAPs. NIH3T3 cells respectively expressing the FAPs of **d** and **e** were mixed 1:1 and imaged using 10 nM MG-2p and 40 nM TO1-2p. The transparency of surface-labeled cells allows fine discrimination of contact surfaces between cells of different colors. Scale bars, 10 μm.

insertion into the cell wall[14]. Live cell imaging using fluorescent proteins fused to GPIs or GPI-anchored proteins is useful for studying organization and function of membrane proteins, including signaling receptors and cell adhesion molecules, but these constructs may also label cell structures involved in biosynthesis, secretion and degradation. Dynamic imaging of lipid rafts and other surface features would benefit by confining fluorescence to proteins anchored to the outer leaflet . Whereas methods such as total internal reflection fluorescence microscopy have evolved to allow selective observation, there are no methods for selective labeling and homogenous detection. To illustrate such labeling and detection, we imaged an MG FAP and an identically anchored AGA2-GFP fusion protein[24] (**Fig. 3b**). The MG FAP and the GFP were visualized on the extracellular surface, but intracellular structures, many with the morphology expected of vacuoles and nuclear membranes (endoplasmic reticulum), were visualized only by the GFP.

To explore fluorogenic labeling of mammalian cell surface proteins, we fused selected TO1 and MG FAPs to the N terminus of platelet-derived growth factor receptor (PDGFR) transmembrane domain. The TO1 and MG FAPs were than expressed stably in NIH3T3 mouse fibroblasts and in M21 human renal carcinoma

cells. In each case the transfected cells exhibited strong surface fluorescence when exposed to low concentrations of TO1-2p or MG-11p fluorogen (**Fig. 3c–f**). No significant intracellular fluorescence was observed under these experimental conditions; TO1-2p and MG-11p controls did not enter living NIH3T3 cells (**Supplementary Fig. 6** online and data not shown).

It is noteworthy that little or no photobleaching of cell surface fluorescence was observed. Separate experiments showed that TO1-2p FAPs resisted bleaching about as well as EGFP and that MG FAPs were even more bleach resistant (**Supplementary Fig. 7** online). Fluorescence signal of TO1-2p FAPs decayed to a TO1-2p concentration-dependent steady state, suggesting that rapid exchange of fluorogen (and/or fluorogen photoproducts) between the solution and the FAP itself was effectively buffering the system against photobleaching. For MG FAPs, other mechanisms may contribute, such as loose sequestration of dark fluorogen on the plasma membrane outer surface.

In aqueous solution mobile fluorogens such as MG or TO1 show almost no photoreactivity[25], but under illumination MG conjugated to an antibody generates reactive oxygen species at a rate similar to GFP[26], sufficient to be phototoxic under continuous or intense excitation[27]. Phototoxicity correlates with photobleaching, suggesting that MG and TO1 FAPs generated reactive oxygen species at GFP-like rates. MG has also been used as an antifungal agent; at experimental concentrations the MG derivatives studied here had little or no effect on yeast growth (**Supplementary Fig. 8** online).

Cell surface-exposed FAPs visualized with a membrane-impermeant fluorogen were seen at the plasma membrane only. When exposed to a membrane-permeant fluorogen, however, these same cells showed additional fluorescence within elements of the secretory apparatus, including the nuclear endoplasmic reticulum and the Golgi (**Fig. 3c** and controls in **Supplementary Fig. 6** online). This result suggests that permeant fluorogens can be used to visualize FAPs shortly after cotranslational insertion into the lumen, and thus potentially report protein folding in near real time. Permeant fluorogens can be added and withdrawn at will, facilitating development of pulse-chase and other approaches to studying secretory and endocytic pathways.

When incorporated into fusion proteins, FAP domains provided a reporter of protein location and abundance in time and space. Fluorescence signal was generated only upon addition of a second component (the fluorogen); in this respect FAPs resemble the site-specific chemical labeling systems. However, all chemical labeling systems require additional manipulation such as enzymatic conjugation steps or washes to reduce background signal, whereas FAPs can be visualized directly after fluorogen addition on a time scale of seconds (on the cell surface) to minutes (within the secretory apparatus). Fluorescence visualization can also be spatially controlled by the appropriate choice of fluorogen, enabling one to selectively observe fusion proteins at particular cellular locations. Multicolor imaging of spectrally and antigenically distinct FAPs co-expressed within a cell will greatly enhance the usefulness of different fluorogens to dynamically monitor complex cellular functions.

ScFv-based FAPs contain internal disulfide linkages and are currently adapted for use only in nonreducing environments, mainly the cell surface and secretory apparatus. FAP/fluorogens thus complement the biarsenical system, which is generally limited to intracellular reducing environments, primarily the cytoplasmic and nuclear compartments[6,7,10]. However, it has been shown that functional scFvs can be expressed cytoplasmically in a disulfide-free format in yeast and mammalian cells[28–30], and future developments of scFv and other FAP platforms will address these intracellular compartments.

## METHODS

Experimental procedures and data analyses are presented as 'Methods and Supplementary Figures' in **Supplementary Materials** online. Methods are described for:

FAP nomenclature; yeast display library and yeast strains[14]; cloning of single chain antibody FAPs[14]; sequencing and classification of FAPs[19]; spectral characterization of yeast surface displayed FAPs; directed evolution of HL1-TO1[20]; secretion and purification of soluble FAPs; fluorogen binding affinity to yeast surface displayed FAPs[20,31]; fluorogen binding affinity to soluble FAPs[31]; quantum yields of FAP/fluorogens[32–35]; corrected absorbance of FAP/fluorogens; fluorogenic enhancement of FAP/fluorogens; mammalian cell surface expression of FAP molecules; microscopy; syntheses of fluorogens[36].

**Accession numbers.** GenBank: EU309680-EU309689.

*Note: Supplementary information is available on the Nature Biotechnology website.*


### ACKNOWLEDGMENTS

We thank Dane Wittrup for providing an aliquot of the yeast scFv surface display library, members of his laboratory for advice and Nicholas Bateman for work on scFv maturation. Supported by National Institutes of Health grant 7 U54 RR022241 and Pennsylvania Department of Health grant 4100020575.


### AUTHOR CONTRIBUTIONS

B.A.S. synthesized fluorogens and derivatives; C.S.-G. and Y.C. cloned fluorogenic scFvs under the direction of C.S.-G.; K.L.Z. carried out cloning-related molecular biology and protein purification; under the direction of J.W.J., S.A. constructed mammalian expression vectors with contribution from K.V.V.; G.W.F. and Q.Y. created stable mammalian cell lines; G.W.F. and J.A.J.F. performed microscopy; C.A.W. implemented directed evolution mutagenesis with contribution from P.B.B.; C.S.-G. conducted spectroscopy and binding experiments and analysis; C.S.-G. drafted manuscript and figures; M.P.B., J.W.J., P.B.B. and A.W. contributed editorially to manuscript and to general design of research; A.W. conceived fluorogen strategy and oversaw entire project.

Published online at http://www.nature.com/naturebiotechnology/
Reprints and permissions information is available online at http://npg.nature.com/reprintsandpermissions


1. Giepmans, B.N., Adams, S.R., Ellisman, M.H. & Tsien, R.Y. The fluorescent toolbox for assessing protein location and function. *Science* **312**, 217–224 (2006).
2. Yao, J., Munson, K.M., Webb, W.W. & Lis, J.T. Dynamics of heat shock factor association with native gene loci in living cells. *Nature* **442**, 1050–1053 (2006).
3. Miesenbock, G., De Angelis, D.A. & Rothman, J.E. Visualizing secretion and synaptic transmission with pH-sensitive green fluorescent proteins. *Nature* **394**, 192–195 (1998).
4. Pertz, O., Hodgson, L., Klemke, R.L. & Hahn, K.M. Spatiotemporal dynamics of RhoA activity in migrating cells. *Nature* **440**, 1069–1072 (2006).
5. Marks, K.M. & Nolan, G.P. Chemical labeling strategies for cell biology. *Nat. Methods* **3**, 591–596 (2006).
6. Adams, S.R. *et al.* New biarsenical ligands and tetracysteine motifs for protein labeling in vitro and in vivo: synthesis and biological applications. *J. Am. Chem. Soc.* **124**, 6063–6076 (2002).
7. Martin, B.R., Giepmans, B.N., Adams, S.R. & Tsien, R.Y. Mammalian cell-based optimization of the biarsenical-binding tetracysteine motif for improved fluorescence and affinity. *Nat. Biotechnol.* **23**, 1308–1314 (2005).
8. Rozinov, M.N. & Nolan, G.P. Evolution of peptides that modulate the spectral qualities of bound, small-molecule fluorophores. *Chem. Biol.* **5**, 713–728 (1998).
9. Farinas, J. & Verkman, A.S. Receptor-mediated targeting of fluorescent probes in living cells. *J. Biol. Chem.* **274**, 7603–7606 (1999).
10. Hauser, C.T. & Tsien, R.Y. A hexahistidine-Zn2+-dye label reveals STIM1 surface exposure. *Proc. Natl. Acad. Sci. USA* **104**, 3693–3697 (2007).
11. Keppler, A. *et al.* A general method for the covalent labeling of fusion proteins with small molecules *in vivo*. *Nat. Biotechnol.* **21**, 86–89 (2003).
12. Chen, I., Howarth, M., Lin, W. & Ting, A.Y. Site-specific labeling of cell surface proteins with biophysical probes using biotin ligase. *Nat. Methods* **2**, 99–104 (2005).
13. Reck-Peterson, S.L. *et al.* Single-molecule analysis of dynein processivity and stepping behavior. *Cell* **126**, 335–348 (2006).
14. Feldhaus, M.J. *et al.* Flow-cytometric isolation of human antibodies from a nonimmune *Saccharomyces cerevisiae* surface display library. *Nat. Biotechnol.* **21**, 163–170 (2003).
15. Nygren, J., Svanvik, N. & Kubista, M. The interactions between the fluorescent dye thiazole orange and DNA. *Biopolymers* **46**, 39–51 (1998).
16. Babendure, J.R., Adams, S.R. & Tsien, R.Y. Aptamers switch on fluorescence of triphenylmethane dyes. *J. Am. Chem. Soc.* **125**, 14716–14717 (2003).

17. Iwaki, T., Torigoe, C., Noji, M. & Nakanishi, M. Antibodies for fluorescent molecular rotors. *Biochemistry* **32**, 7589–7592 (1993).
18. Siegel, R.W., Coleman, J.R., Miller, K.D. & Feldhaus, M.J. High efficiency recovery and epitope-specific sorting of an scFv yeast display library. *J. Immunol. Methods* **286**, 141–153 (2004).
19. Giudicelli, V. *et al.* IMGT/LIGM-DB, the IMGT comprehensive database of immunoglobulin and T cell receptor nucleotide sequences. *Nucleic Acids Res.* **34**, D781–D784 (2006).
20. Colby, D.W. *et al.* Engineering antibody affinity by yeast surface display. *Methods Enzymol.* **388**, 348–358 (2004).
21. Patterson, G.H., Knobel, S.M., Sharif, W.D., Kain, S.R. & Piston, D.W. Use of the green fluorescent protein and its mutants in quantitative fluorescence microscopy. *Biophys. J.* **73**, 2782–2790 (1997).
22. Simeonov, A. *et al.* Blue-fluorescent antibodies. *Science* **290**, 307–313 (2000).
23. Shaner, N.C. *et al.* Improved monomeric red, orange and yellow fluorescent proteins derived from Discosoma sp. red fluorescent protein. *Nat. Biotechnol.* **22**, 1567–1572 (2004).
24. Huang, D. & Shusta, E.V. Secretion and surface display of green fluorescent protein using the yeast *Saccharomyces cerevisiae*. *Biotechnol. Prog.* **21**, 349–357 (2005).
25. Baptista, M.S. & Indig, G.L. Effect of BSA binding on photophysical and photochemical properties of triarylmethane dyes. *J. Phys. Chem. B* **102**, 4678–4688 (1998).
26. Surrey, T. *et al.* Chromophore-assisted light inactivation and self-organization of microtubules and motors. *Proc. Natl. Acad. Sci. USA* **95**, 4293–4298 (1998).
27. Remington, S.J. Fluorescent proteins: maturation, photochemistry and photophysics. *Curr. Opin. Struct. Biol.* **16**, 714–721 (2006).
28. Colby, D.W. *et al.* Development of a human light chain variable domain (V(L)) intracellular antibody specific for the amino terminus of huntingtin via yeast surface display. *J. Mol. Biol.* **342**, 901–912 (2004).
29. Tanaka, T., Lobato, M.N. & Rabbitts, T.H. Single domain intracellular antibodies: a minimal fragment for direct in vivo selection of antigen-specific intrabodies. *J. Mol. Biol.* **331**, 1109–1120 (2003).
30. Proba, K., Worn, A., Honegger, A. & Pluckthun, A. Antibody scFv fragments without disulfide bonds made by molecular evolution. *J. Mol. Biol.* **275**, 245–253 (1998).
31. Motulsky, H. & Christopoulos, A.. *Fitting Models to Biological Data Using Linear and Nonlinear Regression: A Practical Guide to Curve Fitting.* (Oxford University Press, Oxford; New York, 2004).
32. Kubin, R.F. & Fletcher, A.N. Fluorescence quantum yields of some rhodamine dyes. *J. Lumin.* **27**, 455–462 (1982).
33. Lacowicz, J. *Principles of Fluorescence Spectroscopy* edn 2. (Kluwer Academic/Plenum, London, 1999).
34. Mujumdar, R.B., Ernst, L.A., Mujumdar, S.R., Lewis, C.J. & Waggoner, A.S. Cyanine dye labeling reagents: sulfoindocyanine succinimidyl esters. *Bioconjug. Chem.* **4**, 105–111 (1993).
35. Sims, P.J., Waggoner, A.S., Wang, C.H. & Hoffman, J.F. Studies on the mechanism by which cyanine dyes measure membrane potential in red blood cells and phosphatidylcholine vesicles. *Biochemistry* **13**, 3315–3330 (1974).
36. Mueller, W.H.I., Schuetz, H.J. & Meyer, G. Polyethylene glycol derivatives of base and sequence specific DNA ligands: DNA interaction and application for base specific separation of DNA fragments by gel electrophoresis. *Nucleic Acids Res.* **95**, 95–119 (1981).